Biochemical Pharmacology 118 (2016) 59–67

Contents lists available at ScienceDirect

Biochemical Pharmacology

journal homepage: www.elsevier.com/locate/biochempharm

GYY4137 ameliorates intestinal barrier injury in a mouse model of endotoxemia

Shanwen Chen [a], Dingfang Bu [b], Yuanyuan Ma [c], Jing Zhu [a], Lie Sun [a], Shuai Zuo [a], Ju Ma [a], Tengyu Li [a], Zeyang Chen [a], Youwen Zheng [a], Xin Wang [a], Yisheng Pan [a], Pengyuan Wang [a,*], Yucun Liu [a,*]

[a] Division of General Surgery, Peking University First Hospital, Peking University, 8 Xi ShiKu Street, Beijing 100034, People's Republic of China
[b] Central Laboratory, Peking University First Hospital, Peking University, 8 Xi ShiKu Street, Beijing 100034, People's Republic of China
[c] Animal Experiment Center, Peking University First Hospital, Peking University, 8 Xi ShiKu Street, Beijing 100034, People's Republic of China

ARTICLE INFO

Article history:
Received 11 May 2016
Accepted 15 August 2016
Available online 20 August 2016

Keywords:
GYY4137
Hydrogen sulfide
LPS
Tight junction
NF-kB

ABSTRACT

Intestinal barrier injury has been reported to play a vital role in the pathogenesis of endotoxemia. This study aimed to investigate the protective effect of GYY4137, a newly synthesized H_2S donor, on the intestinal barrier function in the context of endotoxemia both *in vitro* and *in vivo*. Caco-2 (a widely used human colon cancer cell line in the study of intestinal epithelial barrier function) monolayers incubated with lipopolysaccharide (LPS) or TNF-α/IFN-γ and a mouse model of endotoxemia were used in this study.

The results suggested that GYY4137 significantly attenuated LPS or TNF-α/IFN-γ induced increased Caco-2 monolayer permeability. The decreased expression of TJ (tight junction) proteins induced by LPS and the altered localization of TJs induced by TNF-α/IFN-γ was significantly inhibited by GYY4137; similar results were obtained *in vivo*. Besides, GYY4137 promoted the clinical score and histological score of mice with endotoxemia. Increased level of TNF-α/IFN-γ in the plasma and increased apoptosis in colon epithelial cells was also attenuated by GYY4137 in mice with endotoxemia. This study indicates that GYY4137 preserves the intestinal barrier function in the context of endotoxemia via multipathways and throws light on the development of potential therapeutic approaches for endotoxemia.

1. Introduction

Sepsis remains a leading cause of death in critically ill patients, the most common kind of which is caused by infection with Gram-negative bacteria, featured by increased level of lipopolysaccharide (LPS) in the blood, also known as endotoxemia [1]. Previous reports have revealed the vital role of intestinal barrier injury in the gut derived infection and the consequent septic multiple organ dysfunction in the pathogenesis of endotoxemia [2,3]. The intestinal barrier is mainly determined by tight junctions (TJs), which function as a physical barrier between the luminal content and the internal milieu [4]. Previous studies have reported that LPS was able to induce decreased expression of TJ proteins and altered localization of TJs via NF-KB mediated MLCK-P-MLC2 signaling, leading to the increased flux of noxious antigens in the lumen into the internal milieu, providing "fuel" for the unremitting inflammatory responses both locally and systematically [5–9].

Hydrogen sulfide (H_2S) has been validated as the third "gasotransmitter" after carbon monoxide and nitric oxide [10,11]. The physiological function of H_2S can be complex, including vasodilation, anti-inflammation and protecting gastric mucosal integrity [12–14]. In the previous reports from our laboratory and others, sodium hydrosulfide (NaHS) has been widely used as a donor to release H_2S [15–17]. However, recent studies suggested that NaHS released large amounts of H_2S over a few seconds under physiological conditions, which mimicked the toxic instead of the physiologic effects of H_2S [18]. As a new synthetic compound, GYY4137 in aqueous solution was found to be able to release lower concentrations of H_2S over longer time periods and thus was used in multiple studies regarding the effects of H_2S [19,20]. However, the effect of GYY4137 on the intestinal barrier function in endotoxemia and the underlying mechanisms have not been illustrated.

The current study indicates that GYY4137 preserves the intestinal barrier function in the context of endotoxemia via multipathways and throws light on the development of potential therapeutic approaches for endotoxemia.

* Corresponding authors at: Division of General Surgery, Peking University First Hospital, Peking University, 8 Xi ShiKu Street, Beijing 100034, People's Republic of China.

E-mail addresses: wangpengyuan2014@126.com (P. Wang), yucunliu@bjmu.edu.cn (Y. Liu).

http://dx.doi.org/10.1016/j.bcp.2016.08.016
0006-2952/

2. Materials and methods

2.1. Reagents

LPS (Escherichia coli serotype 055:B7), GYY4137, FITC-Dextran (4000 Da, FD-4) was purchased from Sigma Aldrich (USA). TNF-α and IFN-γ was purchased from Pepro Tech (USA). Antibodies against ZO-1, Occludin, Alex flour 488 conjugated goat-anti rabbit antibodies and Alex flour 555 conjugated goat-anti mouse antibodies were purchased from Thermo Fisher (USA). Antibodies against Claudin-1, MLCK, MLC2, P-MLC2 and GAPDH were purchased from CST (USA).

2.2. Cell culture

Caco-2 cells were purchased from ATCC (American Type Culture Collection, USA) and maintained at 37 °C in a culture medium as previously described [21,22]. Caco-2 cells were used between passages 28 and 34 in this study. For growth on filters, 10^5 cells were plated on transwell filters with 0.4 μm pore size (Corning Incorporated, USA). The medium involving 10 ng/ml LPS, 10 ng/ml TNF-α/IFN-γ or 50 μM GYY4137 was added to the basolateral compartments.

2.3. Transepithelial Electrical Resistance (TEER) measurements

Caco-2 cells were seeded in 12 well transwell systems and the changes of TEER were measured with an epithelial voltohmmeter ERS-2 (Merck Millipore, USA) as previously reported [23,24]. About 3 weeks after confluence when the filter-grown Caco-2 monolayers reached epithelial resistance of at least 500 Ω cm^2 [25], the cells were incubated with different reagents as indicated. Electrical resistance was measured until similar values were recorded on three consecutive measurements.

2.4. Fluorescein isothiocyanate–dextran 4000 Da (FD-4) Flux assays

Paracellular permeability was assessed following a previously reported method [26,27]. After treatment, Caco-2 monolayers were rinsed with PBS and incubated in the upper chamber with Hank's balanced salt solution containing 1 mg/mL FD-4 solution for 2 h. FD-4 flux was assessed by taking 100 μL from the basolateral chamber. Fluorescent signal was measured with Synergy H_2 microplate reader (Biotek Instruments, USA) using 492 nm excitation and 520 nm emission filters. FD-4 concentrations were determined using standard curves generated by serial dilution.

2.5. Western blot analysis of protein expression

The total protein of the filter grown Caco-2 monolayers was extracted using the method as described previously [11]. The mucosa (2 cm) of proximal colon was collected and total protein was extracted as described previously with little modifications [9]. The extracts containing equal quantities of proteins (30 μg) were electrophoresed in 10% polyacrylamide gel. Subsequently, the separated proteins were transferred onto a PVDF membrane. The membrane was blocked for non-specific binding for 1 h (5% bovine serum albumin (BSA) in TBS-Tween 20 buffer) at room temperature, and then incubated overnight at 4 °C with primary antibodies (1:1000 dilution). The membrane was subsequently incubated at room temperature for 1 h with secondary antibodies. Blots were then developed with electrochemiluminescence (ECL) detection reagents (Merck Millipore, USA).

2.6. Immunofluorescent localization of ZO-1, Occludin and NF-kB p65 in Caco-2 monolayers

Cellular localization of ZO-1, Occludin and NF-kB p65 was assessed by an immunofluorescent antibody labeling technique as previously described [11]. The fluorescence was visualized under Fluoview 1000 confocal microscope (Olympus, Japan).

2.7. Electrophoretic mobility shift assay (EMSA)

Nuclear protein extracts were prepared according to the manufacturer's instructions (Thermo Pierce, USA) and DNA-protein binding assays were carried out by DIG Gel Shift Kit (Roche, Germany) following the manufacturer's recommendations. Double stranded complementary oligonucleotides containing the NF-kB p65 binding sites were synthesized and end-labeled with DIG: 5′-AGTTGAGGGGACTTTCCCAGGC-3′.

2.8. Animals

This study was performed following the guidelines of the China Laboratory Animal Management Committee and the study has been approved by the institute review board at Peking University First Hospital. Male C57BL/6 mice (8 weeks old) were purchased from Vital River Inc. (Beijing, China) and raised in the containment unit of the Laboratory Animal Center at the Peking University First Hospital with access to water and food *ad libitum*. The mice were allowed to adapt to the environment for 1 week before any treatment. The mice were anesthetized with pentobarbital after a specified protocol.

The mouse model of endotoxemia was constructed by intraperitoneal injection of 10 mg/kg LPS. 72 mice were randomly divided into 4 groups: Control; GYY4137 alone; LPS; LPS + GYY4137. Mice in the control group were treated with PBS. Mice in the GYY4137 group were intraperitoneally injected with 50 mg/kg GYY4137. Mice in the LPS group were intraperitoneally injected with 10 mg/kg LPS. Mice in the LPS + GYY4137 group were intraperitoneally injected with 10 mg/kg LPS and 50 mg/kg GYY4137 at baseline. All mice were euthanized 12 h after treatment.

2.9. Clinical assessment

The clinical status of mice in different groups (18 per group) were evaluated utilizing an established clinical score system as

Table 1
Clinical scoring system.

Variable	Score		
	0	1	2
Conjunctivitis	Eyes closed or bleared with serous discharge	Eyes opened with serous discharge	Normal, no conjunctivitis
Stool consistency	Diarrhea	Loose stool	Normal stool
Hair coat	Rough and dull fur, ungroomed	Reduced grooming, rough hair coat	Well groomed, shiny fur
Activity upon moderate stimulation	Lethargic, only lifting of the head after moderate stimulation	Inactive, less alert, <2 steps after moderate stimulation	Normal locomotion and reaction, >2 steps

Table 2
Histological scoring system.

Grade	Histological characteristic(s)
0	Normal mucosal villi
1	Subepithelial Gruenhagen's space (edema), usually at the apex of the villus
2	Extension of the subepithelial space with moderate lifting of epithelial layer from the lamina propria
3	Massive epithelial lifting down the sides of villi; a few tips may be denuded
4	Denuded villi with lamina propria and dilated capillaries exposed
5	Digestion and disintegration of lamina propria; hemorrhage and ulceration

described previously [28]. The scoring system is exhibited in Table 1. Grading was performed in a blinded fashion by 3 independent researchers.

2.10. Histological assessment

The proximal colons (3 per group) collected from mice in different groups were excised and embedded in paraffin. Sections (4 μm) were cut and stained with hematoxylin and eosin (H&E). Images were obtained using a Zeiss Image light microscope at 20× magnification. For each slide, at least 6 images were collected. The degree of histopathologic changes was evaluated by 3 pathologists blinded to the grouping and graded according to a scoring system as described previously [29] (Table 2).

2.11. Measurement of intestinal barrier function

The intestinal barrier function was measured as described previously. Briefly, 12 h after treatment, mice from each group (6 per group) were anesthetized with pentobarbital sodium. A midline laparotomy was performed and a 5 cm segment of distal ileum was isolated with silk ties. 25 mg FD-4 buffered with 0.1 ml PBS was injected into the isolated ileum. The ileum was then placed back into the abdominal cavity and the skin was closed. The abdomen was then covered with a warm wet gauze and the mice was placed on a heated panel and kept under general anesthesia for 30 min. Blood was collected via cardiac puncture and stored in EDTA-coated tubes and centrifuged at 3000 rpm for 15 min at 4 °C. The concentration of FD-4 in the plasma was determined using Synergy H2 microplate reader (Biotek Instruments, USA) using 492 nm excitation and 520 nm emission filters. FD-4 concentrations were determined using standard curves generated by serial dilution.

2.12. Immunofluorescence of ZO-1 and Occludin in frozen proximal colon sections

Proximal colons (3 per group) collected from each group were frozen in optimum cutting temperature compound (OCT) at −80 °C. Sections (4 μm) were cut and immunofluorescent staining was performed as described previously [30]. The fluorescence was visualized under Fluoview 1000 confocal microscope (Olympus, Japan).

2.13. Transmission Electron Microscopy of TJ in colon epithelium

2 mm sections of colon were washed (3 per group) and fixed with 4% glutaraldehyde overnight at 4 °C and then post-fixed with 1% osmium tetroxide. Tissues were embedded in EMbed 812 and thinly sectioned. Sections were then stained with uranyl acetate and lead citrate and examined with an H-450 (Hitachi, Japan) transmission electron microscope.

2.14. Measurement of plasma TNF-α and IFN-γ

The concentrations of TNF-α and IFN-γ in the plasma of mice in different groups (6 per group) were measured with the Quantikine® ELISA kit (R&D, USA) following the manufacturer's recommendations.

2.15. TUNEL analysis

Proximal colons (2 cm) (3 per group) were collected and paraffin-embed and cut into 4 μm sections. TUNEL analysis was carried out utilizing the In Situ Cell Death Detection Kit (POD) following the manufacturer's instructions (Roche, Germany). Images were collected with a Zeiss Image light microscope and the number of apoptotic cells and the total cell number per field in each slide were counted. A minimum of 500 cells and 4 high-powered fields were counted per slide.

The apoptosis index (AI) was calculated according to the following formula:

$$AI = [\text{the number of apoptotic cells}]/[AC + \text{the number of intact cells}] \times 100.$$

2.16. Statistical analysis

The results were expressed as mean ± standard error of the mean (SEM) and analyzed using Student *t* tests for unpaired data and ANOVA to compare groups whenever required (GraphPad Prism version 5.0, CA). A P value < 0.05 was used to indicate statistical significance.

3. Results

3.1. GYY4137 preserved the Caco-2 monolayer barrier function from the injuries induced by LPS

LPS induced significantly decreased monolayer barrier function, featured by decreased TEER and increased FD-4 flux at day 7 after treatment (Fig. 1A). LPS failed to induce significant changes of Caco-2 monolayer barrier function until 3 days after treatment, which was in accordance with the reports from both ours and other laboratories [7,25]. Co-treatment with GYY4137, however, significantly ameliorated the monolayer barrier injuries induced by LPS (Fig. 1A).

3.2. GYY4137 preserved the Caco-2 monolayer barrier function from the injuries induced by TNF-α/IFN-γ

10 ng/ml TNF-α/IFN-γ induced significantly decreased TEER and increased FD-4 flux after treatment for 48 h. Co-treatment with 50 μM GYY4137 significantly attenuated the monolayer barrier injuries induced by TNF-α/IFN-γ (Fig. 1A).

3.3. GYY4137 inhibited LPS induced decreased expression of TJ proteins

GYY4137 significantly ameliorated the decreased expression of ZO-1, Occludin and Claudin-1 induced by LPS in Caco-2 monolayers (Fig. 1B). The results of immunofluorescence showed that GYY4137 inhibited the decreased staining intensity induced by LPS in the Caco-2 monolayers, which was also in accordance with the results of western-blotting (Fig. 2A).

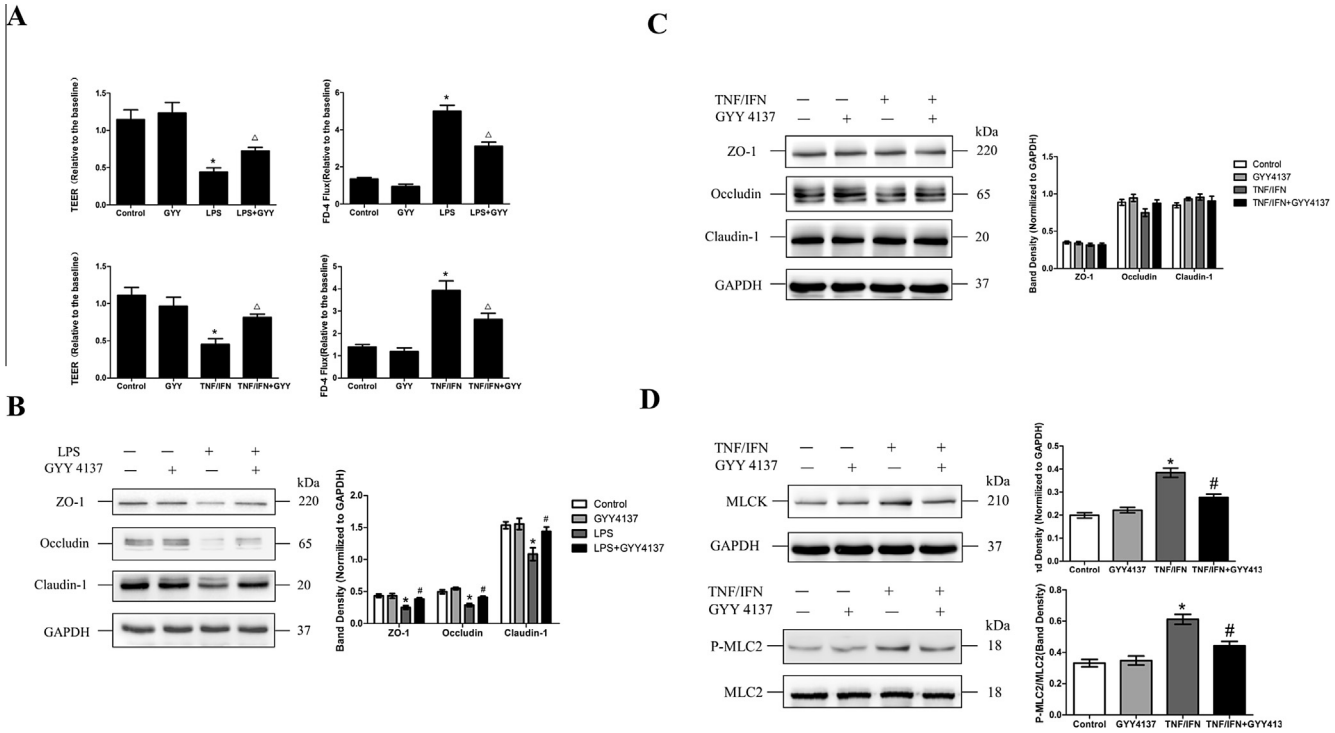

Fig. 1. Protective effect of GYY4137 on LPS and TNF-α/IFN-γ induced Caco-2 monolayer barrier function. A, GYY4137 significantly attenuated the LPS or TNF-α/IFN-γ induced decreased TEER and increased FD-4 flux. Caco-2 monolayers were incubated with 50 μM GYY4137 in the presence or absence of 10 ng/ml LPS, the TEER and FD-4 flux values were collected 7 d after treatment. ($^{*}P < 0.05$, vs control. $^{\#}P < 0.05$ vs LPS) Caco-2 monolayers were incubated with 50 μM GYY4137 in the presence or absence of 10 ng/ml TNF-α and IFN-γ, the TEER and FD-4 flux values were collected 48 h after treatment. ($^{*}P < 0.05$, vs control. $^{\#}P < 0.05$ vs TNF-α/IFN-γ). B, GYY4137 significantly inhibited LPS-induced decreased expression of ZO-1, Occludin and Claudin-1 in Caco-2 monolayers. The total protein of monolayers was collected 7 days after treatment as described in the section of method. ($^{*}P < 0.05$, vs control. $^{\#}P < 0.05$ vs LPS). C, The effect of GYY4137 and TNF-α/IFN-γ on the expression of ZO-1, Occludin and Claudin-1. D, GYY4137 significantly attenuated the increased expression of MLCK and the increased phosphorylation level of MLC2 induced by TNF-α/IFN-γ. ($^{*}P < 0.05$, vs control. $^{\#}P < 0.05$ vs TNF-α/IFN-γ). All experiments were performed in triplicate and repeated at least three times. Results were expressed as mean ± SEM.

3.4. GYY137 attenuated TNF-α/IFN-γ induced activation of MLCK-P-MLC2 signaling via NF-kB p65

GYY4137 or TNF-α/IFN-γ had no significant effect on the expression level of TJ proteins (Fig. 1C). Immunofluorescence of Caco-2 monolayers revealed that TNF-α/IFN-γ induced altered localization of ZO-1 and Occludin, featured by discontinuous and irregular staining compared with control. Co-treatment with GYY4137 remarkably reversed the changes induced by TNF-α/IFN-γ (Fig. 2B). It has been reported that the distribution of TJ proteins was mainly regulated by NF-kB p65 mediated MLCK-P-MLC2 signaling. The results of western blotting showed that the increased expression of MLCK and increased phosphorylation level of MLC2 induced by TNF-α/IFN-γ was significantly attenuated by co-treatment with GYY4137 (Fig. 1D).

EMSA and immunofluorescence suggested that co-treatment with GYY4137 attenuated the increased activation and nuclear localization of NF-kB p65 (Fig. 2C and D).

3.5. GYY4137 improved the clinical and histological status in mice with endotoxemia

The clinical status of mice after injection with or without 10 mg/kg body weight LPS in the presence or absence of 50 mg/kg body weight GYY4137 was evaluated as described previously (Table 1). GYY4137 significantly increased the clinical score of mice with endotoxemia compared with control (Fig. 3A).

The histological status of colon epithelium collected from different groups was evaluated utilizing an established mucosal damage score system (Table 2). Co-treatment with GYY4137 ameliorated the histological damage of colon epithelium in mice with endotoxemia (Fig. 3B and C).

3.6. GYY4137 preserved the intestinal barrier function in mice with endotoxemia

The concentration of FD-4 in the plasma was significantly increased in mice with endotoxemia compared with control. Co-treatment with GYY4137 significantly attenuated the increased level of FD-4 concentration induced by LPS (Fig. 3D). These results indicated that GYY4137 preserved the intestinal barrier function from the injuries induced by LPS in mice with endotoxemia.

3.7. Effect of GYY4137 on the status of TJ proteins and signaling of MLCK-P-MLC2 in mice with endotoxemia

GYY4137 significantly attenuated the decreased expression level of TJ proteins in the proximal colon epithelium of mice with endotoxemia (Fig. 4A). The level of MLCK-P-MLC2 signaling was found to be significantly increased in the proximal colon epithelium of mice with endotoxemia, featured by increased expression level of MLCK and increased phosphorylation level of MLC2 (Fig. 4B). Co-treatment with GYY4137 significantly inhibited the increased signaling of MLCK-P-MLC2 in mice with endotoxemia.

Immunofluorescence of Occludin in the proximal colon epithelium suggested that, in mice with endotoxemia, the staining intensity was markedly decreased compared with control. Co-treatment with GYY4137 ameliorated the change induced by endotoxemia (Fig. 4C).

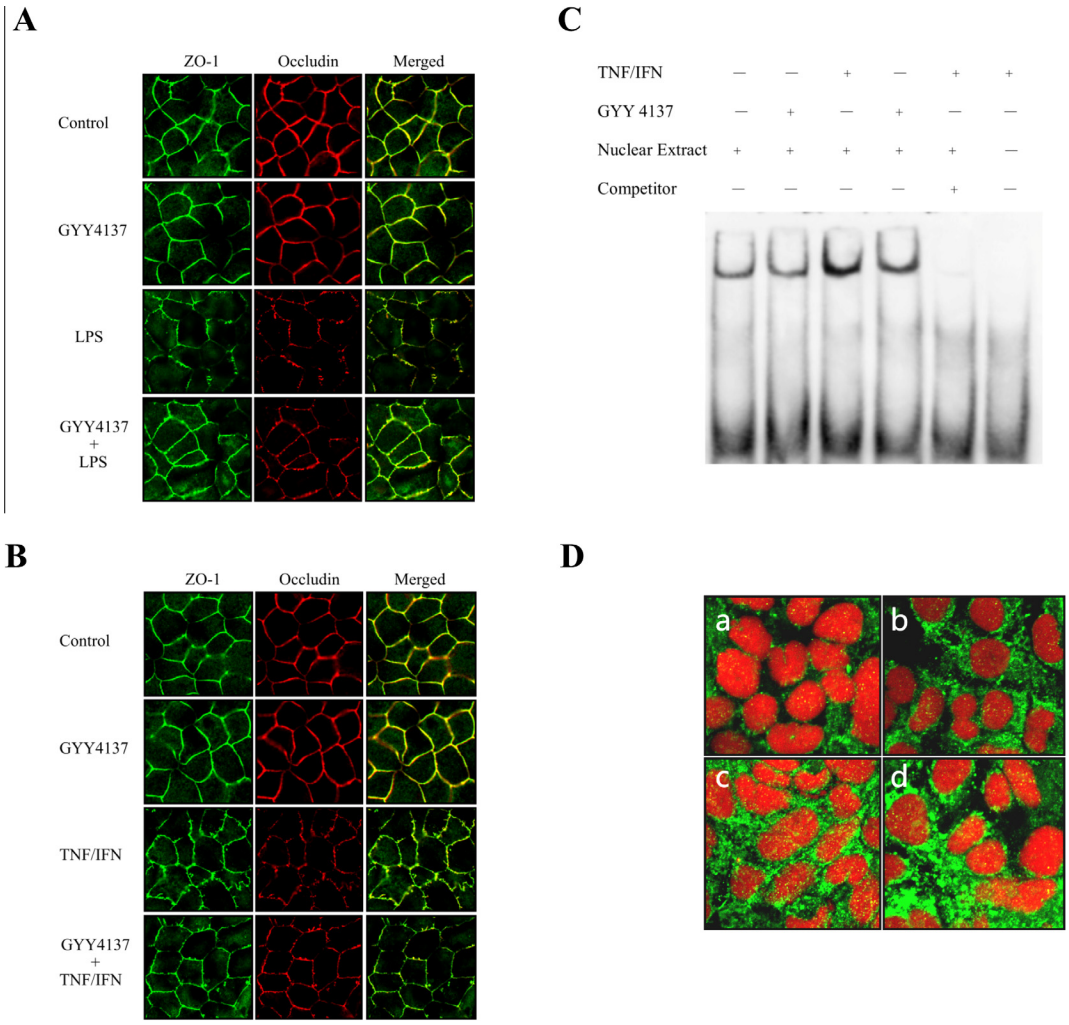

Fig. 2. Immunofluorescence of ZO-1 (green) and Occludin (red) and the status of NF-kB in Caco-2 monolayers. A, Caco-2 monolayers were incubated with 50 μM GYY4137 in the presence or absence of 10 ng/ml LPS for 7 days before the monolayers were fixed (n = 3 for each group). GYY4137 attenuated the LPS induced decreased expression of ZO-1 and Occludin, featured by reduced staining intensity. B, Caco-2 monolayers were exposed to 10 ng/ml TNF-α/IFN-γ for 48 h in the presence or absence of 50 μM GYY4137 for 48 h before monolayers were fixed (n = 3 for each group). GYY4137 ameliorated the altered localization and distribution of ZO-1 and Occludin induced by TNF-α/IFN-γ, featured by discontinuous and irregular staining compared with control. C, Caco-2 monolayers were exposed to 10 ng/ml TNF-α/IFN-γ for 48 h in the presence or absence of 50 μM GYY4137. After treatment, the nuclear extracts of monolayers were harvested. Cold-Probe was added with the nuclear extracts harvested from the monolayers treated with 10 ng/ml TNF-α/IFN-γ to rule out nonspecific conjugation of the labeled probe. D, Caco-2 monolayers were stained for NF-kB p65 by immunofluorescence. Co-treatment with 50 μM GYY4137 significantly inhibited the nuclear translocation of NF-kB p65 elicited by TNF-α/IFN-γ. a: Control; b: Caco-2 monolayers were exposed to 50 μM GYY4137 for 48 h without TNF-α or IFN-γ; c: Caco-2 monolayers were incubated with 10 ng/ml TNF-α/IFN-γ for 48 h; d: Caco-2 monolayers were incubated with 50 μM GYY4137 for 48 h in the presence of 10 ng/ml TNF-α/IFN-γ.

3.8. GYY4137 prevented ultrastructural changes of TJs in mice with endotoxemia

As shown in Fig. 4D, control and GYY4137 mice have an intact structure in the TJs in the colon epithelium. Opened TJs and the decreased electron-dense materials between epithelial cells were observed in the colon epithelium collected from mice with endotoxemia. GYY4137 attenuated the changes of TJs in mice with endotoxemia.

3.9. GYY4137 attenuated the increased plasma level of TNF-α and IFN-γ

GYY4137 significantly attenuated the increased level of TNF-α to around 58% and IFN-γ to around 67% compared with mice with endotoxemia (Fig. 5A and B).

3.10. GYY4137 attenuated the apoptosis of the proximal colon epithelial cells in mice with endotoxemia

As shown in Fig. 5C and D, GYY4137 significantly attenuated the increased TUNEL index in mice with endotoxemia to around 62%, indicating that the inhibition of apoptosis might be one of the mechanisms underlying the effect of GYY4137.

4. Discussion

The intact function of intestinal barrier is mainly determined by TJs, which function as a physical barrier between the lumen and the internal milieu. The "leaky gut", resulting from the decreased intestinal barrier function, played a pivotal role in the pathogenesis of multiple kinds of diseases including endotoxemia by allowing increased flux of noxious antigens into the internal milieu, leading to unremitting inflammatory responses. The increased level of LPS

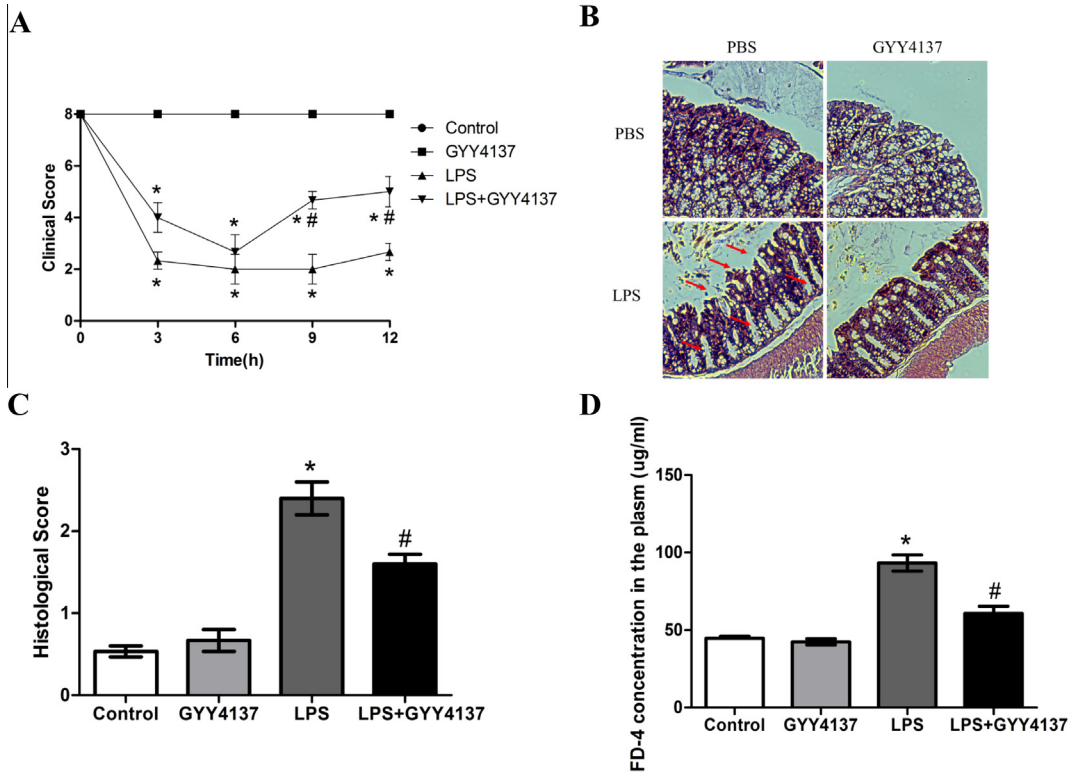

Fig. 3. Effect of GYY4137 on the clinical core, histological score and barrier function of mice with endotoxemia. A, GYY significantly ameliorated the decreased clinical score of mice with endotoxemia. B, Graphs of sections of proximal colon samples. Sections of proximal colon were stained with hematoxylin and eosin (H&E) and viewed using a light microscope (×40). Histological damage is noted in mice with endotoxemia (*Arrows* were added to direct against distinct changes), featured by atrophy of the villi and discrete submucosal. In contrast, less injury was observed in mice with endotoxemia treated with GYY4137 in the same time. C, Colon mucosal damage was assessed utilizing a score system. GYY4137 significantly attenuated the decreased histological score in mice with endotoxemia. D, GYY4137 significantly ameliorated the increased intestinal barrier function featured by increased FD-4 flux in mice with endotoxemia. All experiments were performed with 6 mice per experimental group and repeated at least three times. Results were expressed as mean ± SEM. ($^{*}P < 0.05$, vs control. $^{\#}P < 0.05$ vs LPS).

in the plasma, commonly seen in the context of endotoxemia, has been reported to induce intestinal barrier injury through multiple mechanisms, including decreasing expression of TJ proteins and altering localization of TJs via NF-kB signaling. Upon activation, NF-kB p65 binds to the MLCK promoter region and increases the expression of MLCK mRNA [31,32]. The increased phosphorylation of MLC2 mediated by MLCK leads to contraction of actin-myosin filaments, resulting in altered localization of TJ proteins and consequently, the functional opening of TJs [33,34]. These studies imply the existence of a vicious cycle in the intestinal epithelium consisting of the inflammatory response and the injured intestinal barrier function in the context of endotoxemia. Thus, it remains a promising method for seeking potential therapeutic reagents for endotoxemia by verifying novel regents that may have protective effect on the intestinal barrier function.

GYY4137, as a new kind of H_2S donor, was able to release stable quantities of H_2S in the physiological context in the longer term compared with the traditionally used H_2S donor, NaHS, and thus has been increasingly used as a pharmacological "tool" to investigate the biological functions of H_2S [35]. Li et al. reported that GYY 4137 (50 mg/kg, *i.p.*) was able to generate a stable plasma H_2S level (around 55 μmol/L) in at least the following 3 h after treatment [36]. The results of following *in vivo* studies in mice and rats also suggested the stability of GYY 4137 as a novel H_2S donor [37–40]. Recently, studies have revealed the anti-inflammatory and anti-apoptosis effect of GYY4137 in multiple kinds of tissues [40,41]. However, the effect of GYY4137 on the intestinal barrier function and the underlying mechanisms has not been illustrated.

In this study, the effect of GYY4137 on the intestinal barrier function was investigated *in vitro* utilizing Caco-2 monolayers. The studies from our laboratory and others have revealed that LPS could cause direct damage to the Caco-2 monolayer barrier function by decreasing the expression of TJ proteins. TNF-α/IFN-γ, however, induced the increased permeability of monolayers by inducing the altered localization of TJs via NF-kB p65 mediated MLCK-P-MLC2 signaling. The combination of these two models of injured intestinal barrier function provided the approach for the investigation of the effect of GYY4137 on both the expression and the distribution of TJ proteins in the context of endotoxemia. The concentrations of LPS (10 ng/ml) and TNF-α (10 ng/ml)/IFN-γ (10 ng/ml) used in this study were at clinically related concentrations in the context of endotoxemia according to the previous reports [17,25]. The results indicated that GYY4137 preserved the intestinal barrier function from the injuries caused by LPS or TNF-α/IFN-γ by maintaining the function of TJs. EMSA and immunofluorescence suggested that GYY4137 significantly inhibited the activation and increased nuclear localization of NF-kB p65 induced by TNF-α/IFN-γ.

A mouse model of endotoxemia was subsequently constructed by injecting 10 mg/kg body weight LPS i.p. in this study. 50 mg/kg GYY4137 was injected i.p. in the baseline to investigate the effect of GYY4137 on the LPS induced intestinal barrier injury *in vitro*. Considering the pathogenesis of endotoxemia as a systemic disease, the clinical status of mice after different treatment was tested using a scoring system as described previously. GYY4137 significantly improved the overall status of mice with endotoxemia. FD-4 flux assay suggested that GYY4137 was able to attenuate the increased

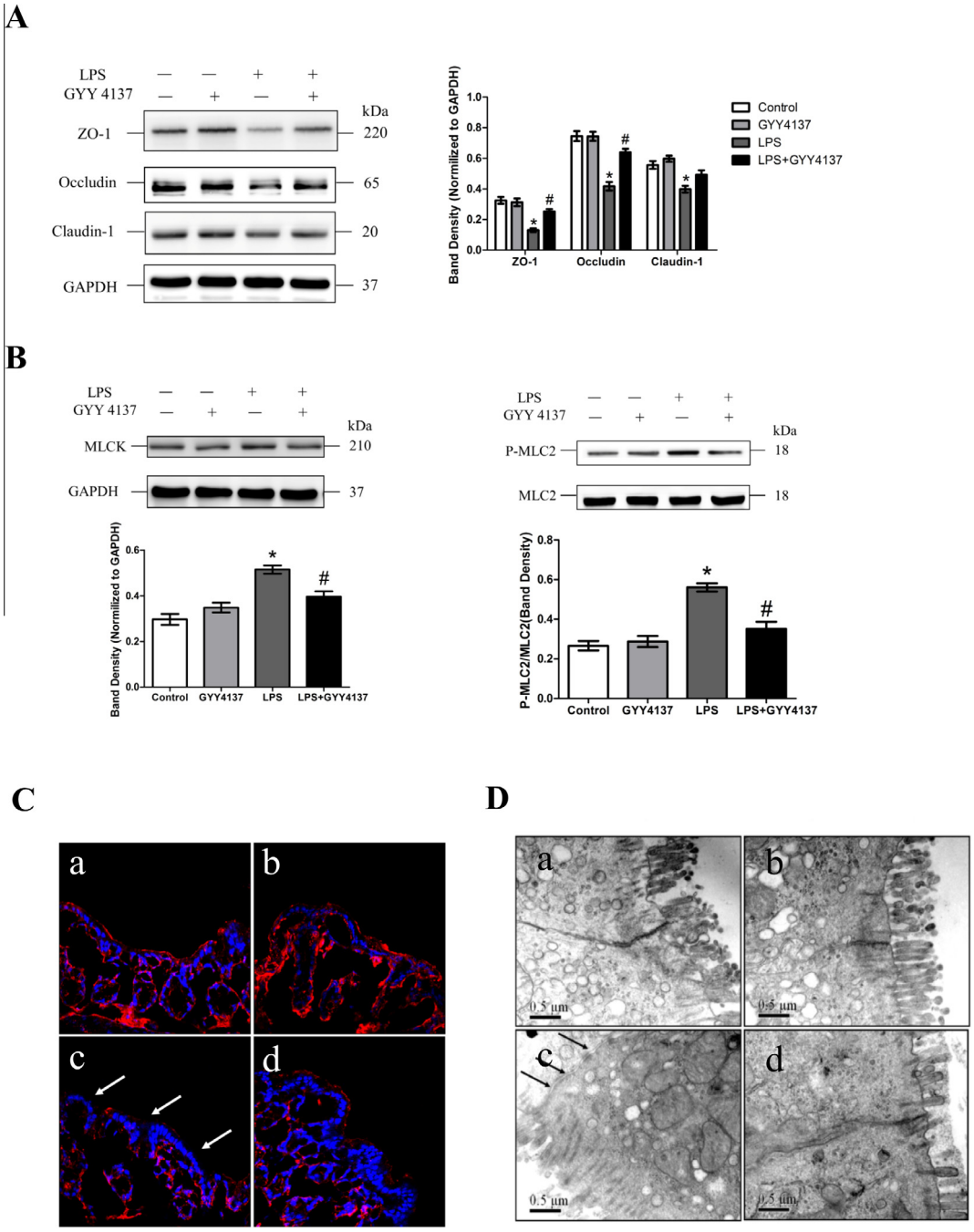

Fig. 4. The effect of GYY4137 on the expression of TJ proteins, the status of MLCK-P-MLC2 signaling and the structure of TJs in mice with endotoxemia. Total protein was collected from the proximal 2 cm colon epithelium from mice in different groups 12 h after injection as described in the section of method. A, GYY4137 significantly inhibited the decreased expression of ZO-1, Occludin and Claudin-1 in the proximal colon epithelium of mice with endotoxemia. B, GYY4137 significantly attenuated the increased expression of MLCK and the increased phosphorylation level of MLC2 in the proximal colon epithelium of mice with endotoxemia. C, Occludin (red) was stained by immunofluorescence as a marker of the changes of TJ proteins in the colon epithelium. a: Control; b: Mice treated with GYY4137 without LPS; c: Mice treated with LPS; d: Mice treated with both LPS and GYY4137. GYY4137 ameliorated the decreased staining intensity of Occludin in mice with endotoxemia (*Arrows* were added to direct against distinct changes). D, Ultrastructure of TJs in colon was observed by TEM. a: Control; b: Mice treated with GYY4137 without LPS; c: Mice treated with LPS; d: Mice treated with both LPS and GYY4137. The TJs were not intact and the electron-dense materials were diminished in mice with endotoxemia. Wider intervals were observed between the epithelial cells in mice with endotoxemia. (*Arrows* were added to direct against distinct changes). All experiments were performed with 6 mice per experimental group and repeated at least three times. Results were expressed as mean ± SEM. ($^{*}P < 0.05$, vs control. $^{\#}P < 0.05$ vs LPS).

colon epithelial permeability in the context of endotoxemia. Histological evaluation of the colon epithelium suggested that GYY4137 exerted protective effect on the structure of the colon epithelium at the histological level. The inhibitory effect of GYY4137 on the signaling pathway of MLCK-P-MLC2 and the decreased expression of TJ proteins was in accordance with the results collected *in vitro* in Caco-2 monolayers. The results of TEM validated the protective effect of GYY4137 on the function of TJs in mice with endotoxemia at the ultrastructural level.

Previous reports have implied the pivotal role of increased level of proinflammatory cytokines including TNF-α/IFN-γ in the pathogenesis of endotoxemia and the consequent multiple organ dysfunction [42,43]. In this study, the results of ELISA suggested that GYY4137 significantly attenuated the increased level of TNF-α

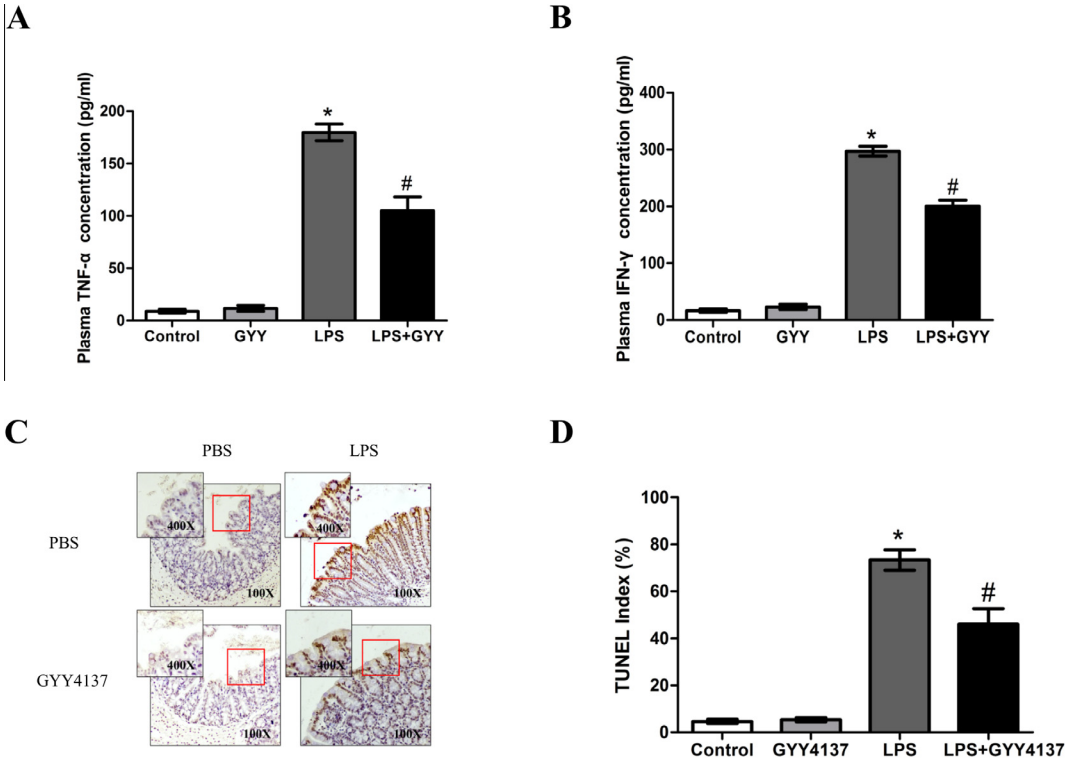

Fig. 5. The effect of GYY4137 on the plasma level of TNF-α and IFN-γ and the level of apoptosis in the proximal colon epithelium in mice with endotoxemia. A, GYY4137 significantly inhibited the increased TNF-α in the plasma of mice with endotoxemia. B, GYY4137 significantly inhibited the increased IFN-γ in the plasma of mice with endotoxemia. C, Representative TUNEL images for cell apoptosis (brawn signals, magnification ×100, ×400). D, Apoptosis index of proximal colon epithelial cells. GYY4137 significantly inhibited the increased level of apoptosis in the colon epithelium in mice with endotoxemia. All experiments were performed with 6 mice per experimental group and repeated at least three times. Results were expressed as mean ± SEM. ($^{*}P < 0.05$, vs control. $^{\#}P < 0.05$ vs LPS).

and IFN-γ in the plasma of mice with endotoxemia, indicating the potential protective effect of GYY4137 on the systemic injuries in the pathogenesis of endotoxemia.

Increased level of apoptosis of intestinal epithelial cells has been considered as an important mechanism underlying the injured intestinal barrier function in the context of endotoxemia [44,45]. In this study, TUNEL analysis suggested that GYY4137 significantly attenuated the increased level of apoptosis in the colon epithelial cells in mice with endotoxemia.

The inhibitory effect of H_2S on the activation of NF-kB observed in the present study was in accordance with the results of plethora of previous studies [16,46]. Sen et al. reported that H_2S acted by sulfhydrating the p65 subunit of NF-kB at cysteine-38, leading to the deceased activation and nuclear translocation of NF-kB [47]. This directly inhibitory effect on the activation of NF-kB might be the pivotal mechanism underlying the anti-inflammatory effect of H_2S in many tissues [48]. Recently, IL-6 and silent information regulator 2 (SIR2) family have also been reported to be involved in the effect of H_2S, which requires further investigation [49,50].

In conclusion, this study illustrates the protective effect of GYY4137 on the intestinal barrier function in the context of endotoxemia both *in vitro* and *in vivo*. Inhibiting NF-kB mediated MLCK-P-MLC2 pathway and apoptosis might be the mechanism underlying the protective effect of GYY4137. The inhibitory effect of GYY4137 on the systemic inflammatory response requires further research and may provide potential therapeutic targets for endotoxemia.

Funding

This work is supported by the grant for the research about the potential therapeutic approaches for surgical infection and the underlying mechanisms from China Health & Medical Development Foundation.

Conflict of interest statement

There is no conflict of interest.

References

[1] R.S. Hotchkiss, I.E. Karl, The pathophysiology and treatment of sepsis, N. Engl. J. Med. 348 (2003) 138–150.
[2] M.P. Fink, Effect of critical illness on microbial translocation and gastrointestinal mucosa permeability, Semin. Respir. Infect. 9 (1994) 256–260.
[3] P. Yu, C.M. Martin, Increased gut permeability and bacterial translocation in Pseudomonas pneumonia-induced sepsis, Crit. Care Med. 28 (2000) 2573–2577.
[4] J.R. Turner, Intestinal mucosal barrier function in health and disease, Nat. Rev. Immunol. 9 (2009) 799–809.
[5] S. Guo, M. Nighot, R. Al-Sadi, T. Alhmoud, P. Nighot, T.Y. Ma, Lipopolysaccharide regulation of intestinal tight junction permeability is mediated by TLR4 signal transduction pathway activation of FAK and MyD88, J. Immunol. 195 (2015) 4999–5010.
[6] D. Song, X. Zong, H. Zhang, et al., Antimicrobial peptide Cathelicidin-BF prevents intestinal barrier dysfunction in a mouse model of endotoxemia, Int. Immunopharmacol. 25 (2015) 141–147.
[7] S.W. Chen, P.Y. Wang, J. Zhu, et al., Protective effect of 1,25-dihydroxyvitamin d3 on lipopolysaccharide-induced intestinal epithelial tight junction injury in caco-2 cell monolayers, Inflammation 38 (2015) 375–383.
[8] X. Zong, W. Hu, D. Song, et al., Porcine lactoferrin-derived peptide LFP-20 protects intestinal barrier by maintaining tight junction complex and modulating inflammatory response, Biochem. Pharmacol. 104 (2016) 74–82.
[9] R. Moriez, C. Salvador-Cartier, V. Theodorou, J. Fioramonti, H. Eutamene, L. Bueno, Myosin light chain kinase is involved in lipopolysaccharide-induced disruption of colonic epithelial barrier and bacterial translocation in rats, Am. J. Pathol. 167 (2005) 1071–1079.
[10] F. Wagner, P. Asfar, E. Calzia, P. Radermacher, C. Szabó, Bench-to-bedside review: hydrogen sulfide – the third gaseous transmitter: applications for critical care, Crit. Care 13 (2009) 213.

[11] R. Wang, Physiological implications of hydrogen sulfide: a whiff exploration that blossomed, Physiol. Rev. 92 (2012) 791–896.
[12] J.L. Kutz, J.L. Greaney, L. Santhanam, L.M. Alexander, Evidence for a functional vasodilatatory role for hydrogen sulphide in the human cutaneous microvasculature, J. Physiol. 593 (2015) 2121–2129.
[13] B. Gemici, J.L. Wallace, Anti-inflammatory and cytoprotective properties of hydrogen sulfide, Methods Enzymol. 555 (2015) 169–193.
[14] M. Magierowski, K. Magierowska, S. Kwiecien, T. Brzozowski, Gaseous mediators nitric oxide and hydrogen sulfide in the mechanism of gastrointestinal integrity, protection and ulcer healing, Molecules 20 (2015) 9099–9123.
[15] C. Gao, D.Q. Xu, C.J. Gao, et al., An exogenous hydrogen sulphide donor, NaHS, inhibits the nuclear factor κB inhibitor kinase/nuclear factor κb inhibitor/nuclear factor-κB signaling pathway and exerts cardioprotective effects in a rat hemorrhagic shock model, Biol. Pharm. Bull. 35 (2012) 1029–1034.
[16] J. Du, Y. Huang, H. Yan, et al., Hydrogen sulfide suppresses oxidized low-density lipoprotein (ox-LDL)-stimulated monocyte chemoattractant protein 1 generation from macrophages via the nuclear factor κB (NF-κB) pathway, J. Biol. Chem. 289 (2014) 9741–9753.
[17] S.W. Chen, J. Zhu, S. Zuo, et al., Protective effect of hydrogen sulfide on TNF-α and IFN-γ-induced injury of intestinal epithelial barrier function in Caco-2 monolayers, Inflamm. Res. 64 (2015) 789–797.
[18] W. Feng, X.Y. Teo, W. Novera, et al., Discovery of new H2S releasing phosphordithioates and 2,3-dihydro-2-phenyl-2 sulfanylenebenzo[d][1,3,2] oxazaphospholes with improved antiproliferative activity, J. Med. Chem. 58 (2015) 6456–6480.
[19] Z. Liu, Y. Han, L. Li, et al., The hydrogen sulfide donor, GYY4137, exhibits anti-atherosclerotic activity in high fat fed apolipoprotein E(−/−) mice, Br. J. Pharmacol. 169 (2013) 1795–1809.
[20] E. Grambow, F. Mueller-Graf, E. Delyagina, M. Frank, A. Kuhla, B. Vollmar, Effect of the hydrogen sulfide donor GYY4137 on platelet activation and microvascular thrombus formation in mice, Platelets 25 (2014) 166–174.
[21] D. Ye, S. Guo, R. Al-Sadi, T.Y. Ma, MicroRNA regulation of intestinal epithelial tight junction permeability, Gastroenterology 141 (2011) 1323–1333.
[22] L.F. Xu, X. Teng, J. Guo, M. Sun, Protective effect of intestinal trefoil factor on injury of intestinal epithelial tight junction induced by platelet activating factor, Inflammation 35 (2012) 308–315.
[23] T.Y. Ma, N. Hoa, D. Tran, et al., Cytochalasin B modulation of Caco-2 tight junction barrier: role of myosin light chain kinase, Am. J. Physiol. Gastrointest. Liver Physiol. 279 (2000) 875–885.
[24] T.Y. Ma, D. Nguyen, V. Bui, et al., Ethanol modulation of intestinal epithelial tight junction barrier, Am. J. Physiol. Gastrointest. Liver Physiol. 276 (1999) 965–974.
[25] S. Guo, R. Al-Sadi, H.M. Said, et al., Lipopolysaccharide causes an increase in intestinal tight junction permeability in vitro and in vivo by inducing enterocyte membrane expression and localization of TLR-4 and CD14, Am. J. Pathol. 182 (2013) 375–387.
[26] N. Schlegel, M. Meir, V. Spindler, C.T. Germer, J. Waschke, Differential role of RhoGTPases in intestinal epithelial barrier regulation in vitro, J. Cell. Physiol. 226 (2011) 1196–1203.
[27] M. Schliwa, Action of cytochalasin D on cytoskeletal networks, J. Cell Biol. 92 (1982) 79–91.
[28] A. Kadl, J. Pontiller, M. Exner, N. Leitinger, Single bolus injection of bilirubin improves the clinical outcome in a mouse model of endotoxemia, Shock 28 (2007) 582–588.
[29] C.J. Chiu, A.H. McArdle, R. Brown, H.J. Scott, F.N. Gurd, Intestinal mucosal lesion in low-flow states. I. A morphological, hemodynamic, and metabolic reappraisal. Intestinal mucosal lesion in low-flow states. I. A morphological, hemodynamic, and metabolic reappraisal, Arch. Surg. 101 (1970) 478–483.
[30] J. Karczewski, F.J. Troost, I. Konings, et al., Regulation of human epithelial tight junction proteins by *Lactobacillus plantarum* in vivo and protective effects on the epithelial barrier, Am. J. Physiol. Gastrointest. Liver Physiol. 298 (2010) 851–859.
[31] T.Y. Ma, M.A. Boivin, D. Ye, A. Pedram, H.M. Said, Mechanism of TNF-α modulation of Caco-2 intestinal epithelial tight junction barrier: role of myosin light-chain kinase protein expression, Am. J. Physiol. Gastrointest. Liver Physiol. 288 (2005) 422–430.
[32] R. Al-Sadi, D. Ye, K. Dokladny, T.Y. Ma, Mechanism of IL-1beta-induced increase in intestinal epithelial tight junction permeability, J. Immunol. 180 (2008) 5653–5661.
[33] L. Shen, E.D. Black, E.D. Witkowski, et al., Myosin light chain phosphorylation regulates barrier function by remodeling tight junction structure, J. Cell Sci. 119 (2006) 2095–2106.
[34] R.H. Ralay, N. Carusio, R. Wangensteen, et al., Protection against endotoxic shock as a consequence of reduced nitrosative stress in MLC2K210-null mice, Am. J. Pathol. 170 (2007) 439–446.
[35] P. Rose, B.W. Dymock, P.K. Moore, GYY4137, a novel water-soluble, H2S-releasing molecule, Methods Enzymol. 554 (2015) 143–167.
[36] L. Li, M. Whiteman, Y.Y. Guan, K.L. Neo, Y. Cheng, S.W. Lee, Y. Zhao, R. Baskar, C. H. Tan, P.K. Moore, Characterization of a novel, water-soluble hydrogen sulfide-releasing molecule (GYY4137): new insights into the biology of hydrogen sulfide, Circulation 117 (18) (2008) 2351–2360.
[37] Z. Liu, Y. Han, L. Li, H. Lu, G. Meng, X. Li, M. Shirhan, M.T. Peh, L. Xie, S. Zhou, X. Wang, Q. Chen, W. Dai, C.H. Tan, S. Pan, P.K. Moore, Y. Ji, The hydrogen sulfide donor, GYY4137, exhibits anti-atherosclerotic activity in high fat fed apolipoprotein E(−/−) mice, Br. J. Pharmacol. 169 (8) (2013) 1795–1809.
[38] E. Grambow, F. Mueller-Graf, E. Delyagina, M. Frank, A. Kuhla, B. Vollmar, Effect of the hydrogen sulfide donor GYY4137 on platelet activation and microvascular thrombus formation in mice, Platelets 25 (3) (2014) 166–174.
[39] S. Lilyanna, M.T. Peh, O.W. Liew, P. Wang, P.K. Moore, A.M. Richards, E.C. Martinez, GYY4137 attenuates remodeling, preserves cardiac function and modulates the natriuretic peptide response to ischemia, J. Mol. Cell. Cardiol. 87 (2015) 27–37.
[40] G. Meng, J. Wang, Y. Xiao, et al., GYY4137 protects against myocardial ischemia and reperfusion injury by attenuating oxidative stress and apoptosis in rats, J. Biomed. Res. 29 (2015) 203–213.
[41] Z. Wu, H. Peng, Q. Du, W. Lin, Y. Liu, GYY4137, a hydrogen sulfide-releasing molecule, inhibits the inflammatory response by suppressing the activation of nuclear factor-kappa B and mitogen-activated protein kinases in Coxsackie virus B3-infected rat cardiomyocytes, Mol. Med. Rep. 11 (3) (2015) 1837–1844.
[42] A. Er, E. Yazar, K. Uney, M. Elmas, F. Altan, G. Cetin, Effects of tylosin on serum cytokine levels in healthy and lipopolysaccharide-treated mice, Acta Vet. Hung. 58 (1) (2010) 75–81.
[43] M. Bosmann, P.A. Ward, The inflammatory response in sepsis, Trends Immunol. 34 (2013) 129–136.
[44] C.M. Coopersmith, P.E. Stromberg, C.G. Davis, W.M. Dunne, D.M. Amiot 2nd, I.E. Karl, R.S. Hotchkiss, T.G. Buchman, Sepsis from *Pseudomonas aeruginosa* pneumonia decreases intestinal proliferation and induces gut epithelial cell cycle arrest, Crit. Care Med. 31 (2003) 1630–1637.
[45] J.M. Williams, C.A. Duckworth, A.J. Watson, et al., A mouse model of pathological small intestinal epithelial cell apoptosis and shedding induced by systemic administration of lipopolysaccharide, Dis. Model Mech. 6 (2013) 1388–1399.
[46] R. Guo, K. Wu, J. Chen, L. Mo, X. Hua, D. Zheng, P. Chen, G. Chen, W. Xu, J. Feng, Exogenous hydrogen sulfide protects against doxorubicin-induced inflammation and cytotoxicity by inhibiting p38MAPK/NF-κB pathway in H9c2 cardiac cells, Cell. Physiol. Biochem. 32 (6) (2013) 1668–1680.
[47] N. Sen, B.D. Paul, M.M. Gadalla, A.K. Mustafa, T. Sen, R. Xu, S. Kim, S.H. Snyder, Hydrogen sulfide-linked sulfhydration of NF-κB mediates its antiapoptotic actions, Mol. Cell 45 (1) (2012) 13–24.
[48] J.L. Wallace, R.W. Blackler, M.V. Chan, G.J. Da Silva, W. Elsheikh, K.L. Flannigan, I. Gamaniek, A. Manko, L. Wang, J.P. Motta, A.G. Buret, Anti-inflammatory and cytoprotective actions of hydrogen sulfide: translation to therapeutics, Antioxid. Redox Signal. 22 (5) (2015) 398–410.
[49] H. Xin, M. Wang, W. Tang, Z. Shen, L. Miao, W. Wu, C. Li, X. Wang, X. Xin, Y.Z. Zhu, Hydrogen sulfide attenuates inflammatory hepcidin by reducing IL-6 secretion and promoting SIRT1-mediated STAT3 deacetylation, Antioxid. Redox Signal. 24 (2) (2016) 70–83.
[50] L. Xie, H. Feng, S. Li, G. Meng, S. Liu, X. Tang, Y. Ma, Y. Han, Y. Xiao, Y. Gu, Y. Shao, C.M. Park, M. Xian, Y. Huang, A. Ferro, R. Wang, P.K. Moore, H. Wang, Y. Ji, SIRT3 mediates the antioxidant effect of hydrogen sulfide in endothelial cells, Antioxid. Redox Signal. 24 (6) (2016) 329–343.